Seasonality of phytoplankton growth limitation by iron and manganese in subantarctic waters

Pauline Latour[1,2,*], Robert F. Strzepek[2,3], Kathrin Wuttig[2], Pier van der Merwe[3], Sam Eggins[4], Lennart T. Bach[1], Philip W. Boyd[1,2,3], Michael J. Ellwood[4], Terry L. Pinfold[5] and Andrew R. Bowie[1,2,3]

[1]*Institute for Marine and Antarctic Studies, University of Tasmania, Locked Bag 129, Hobart, TAS 7001, Australia*

[2]*Antarctic Climate and Ecosystems Cooperative Research Centre (ACE CRC), University of Tasmania, Private Bag 80, Hobart, TAS 7001, Australia*

[3]*Australian Antarctic Program Partnership (AAPP), Institute for Marine and Antarctic Studies, University of Tasmania, Hobart, TAS, 7001, Australia*

[4]*Research School of Earth Sciences, Australian National University, 142 Mills Rd, Acton ACT, Canberra, 0200 Canberra*

[5]*School of Medicine, College of Health and Medicine, University of Tasmania, Hobart, TAS 7000, Australia*

*Corresponding author at: Institute for Marine and Antarctic Studies, University of Tasmania, Locked Bag 129, Hobart, TAS, 7001, Australia.

Email: pauline.latour@utas.edu.au

Keywords: iron; manganese; co-limitation; phytoplankton; Southern Ocean; subantarctic zone, radioisotopes; photophysiology; flow cytometry.

Key findings:

- Seasonality in phytoplankton Fe limitation with the strongest signal in summer
- Mn addition preferentially stimulated the growth of cyanobacteria in autumn
- Combined Fe and Mn additions stimulated nanoplankton carbon fixation in spring and microplankton in summer, suggesting Fe and -Mn co-limited parts of the phytoplankton community

Abstract

Phytoplankton indirectly influence the climate, through their role in the ocean biological carbon pump. Hence factors limiting phytoplankton growth directly impact the strength of the biological carbon pump and consequently climate. In the Southern Ocean, the subantarctic zone represents an important carbon sink, yet variables limiting phytoplankton growth are not fully constrained. Co-limitation by iron (Fe) and manganese (Mn) has recently been observed in the coastal and offshore Southern Ocean, but very few studies have focused on the subantarctic zone. In addition, no study has investigated the seasonal variability of Mn (co-)limitation of phytoplankton growth in the Southern Ocean. Using three shipboard bioassay experiments, we evaluated the seasonality of Fe and Mn co-limitation of subantarctic phytoplankton growth, south of Tasmania. We observed a strong seasonal variation in phytoplankton Fe limitation, and that the response of phytoplankton to Mn was subtle and thus readily masked by the responses to Fe. Combined addition of Fe and Mn enhanced carbon uptake of nanoeukaryotes in spring and microeukaryotes in summer while the addition of Mn alone stimulated the growth of

picocyanobacteria in autumn. These results suggest the importance of Mn may vary seasonally and its control on phytoplankton growth may be associated with specific taxa.

Introduction

Phytoplankton play a major role in the marine carbon cycle by driving the transfer of carbon dioxide from the atmosphere into the ocean through photosynthesis. This process is part of the biological carbon pump, and its strength varies between and within oceanic regions (Lenton et al. 2013; Deppeler and Davidson 2017). The Southern Ocean is comprised of several biogeochemical regions with contrasting hydrographic and nutrient conditions: the subantarctic zone, the polar front zone, the Antarctic zone, and the seasonal sea ice zone, each delimited by fronts (Orsi et al. 1995). South of the subtropical front, phytoplankton growth is mainly limited by very low concentrations of iron (Fe) (Boyd et al. 2000; Deppeler and Davidson 2017). Other factors may also limit phytoplankton growth, such as low light and temperature, or specifically north of the polar front, low silicic acid levels (Boyd 2002; Bowie et al. 2009; Strzepek et al. 2012). These limiting factors (alone or combined) directly impact the strength of regional biological carbon pump and hence need to be identified to project changes to the oceanic carbon cycle during the Anthropocene.

Interest in nutrient co-limitation of Southern Ocean phytoplankton has recently grown (Middag et al. 2013; Browning et al. 2014; Browning et al. 2021). Specifically, several studies have identified Fe and manganese (Mn) co-limitation in both coastal (Wu et al. 2019) and open ocean waters (Browning et al. 2021) of the Southern Ocean. Co-limitation occurs when two or more elements limit phytoplankton growth simultaneously, and several kinds of co-limitation have been identified. Saito et al. (2008) classified Mn co-limitation as a type II "Biochemical substitution co-limitation", in which two elements are expected to substitute for each other for the same active site of an enzyme, for example, Fe and Mn within the superoxide dismutase enzyme. Manganese is an essential element for phytoplankton growth, used in the oxygen-evolving complex for the water-splitting reaction of photosynthesis and in the superoxide dismutase enzyme to defend against reactive oxygen species (ROS) (Sunda et al. 1983; Peers and Price 2004). Therefore, phytoplankton growth may be limited in regions where dissolved Mn (dMn) concentrations are particularly low, such as the Southern Ocean (Westerlund and Öhman 1991; Middag et al. 2011, 2013; Latour et al. 2021). Importantly, phytoplankton Mn requirements may vary depending on Fe conditions. Peers and Price (2004) observed that diatoms increased their Mn content under Fe stress, presumably to produce more superoxide dismutase enzyme to counter the additional ROS production associated with Fe limitation. If Fe limitation increases the cellular requirement for Mn, Mn (co-)limitation may be expected in Southern Ocean phytoplankton limited by Fe (Boyd et al. 2000; Deppeler and Davidson 2017). However, several earlier shipboard incubation experiments in Southern Ocean waters did not observe an effect of Mn addition in either coastal or open waters of the Southern Ocean during the austral spring and summer (Buma et al. 1991; Scharek et al. 1997; Sedwick

et al. 2000), suggesting that Mn (co-)limitation is not pervasive within the Southern Ocean and may vary between regions and seasons.

The subantarctic zone, the northernmost region of the Southern Ocean, sustains the strongest carbon uptake of all the Southern Ocean biogeochemical regions (Lenton et al. 2013). In terms of biology, this region sees the transition from phytoplankton communities containing coccolithophores and fewer diatoms in northern waters towards more diatoms and less coccolithophores in polar waters (Trull et al. 2001). Usually, pico- and nanoplankton dominate phytoplankton communities in terms of cell counts, but high grazing pressure keeps their abundance relatively low with little seasonal variability (Deppeler and Davidson 2017 and references therein). In this region, Fe was demonstrated as the main factor limiting phytoplankton growth, with silicic acid possibly (co-)limiting diatoms (Boyd et al. 1999; Westwood et al. 2011; Eriksen et al. 2018). Until now, the study of Fe-Mn co-limitation of phytoplankton growth has been restricted to a few polar Southern Ocean sites (Buma et al. 1991; Scharek et al. 1997; Sedwick et al. 2000; Wu et al. 2019; Browning et al. 2021), with only the Browning et al. (2021) study looking at potential co-limitation within subantarctic waters. A recent study showed that dMn concentrations are low in subantarctic waters south of Tasmania, with an average concentration of 0.24 nM measured within the surface mixed layer during the austral summer 2018 (Latour et al., 2021). In this region, Mn, like Fe, may be delivered to the ocean through atmospheric inputs from Tasmania and mainland Australia or sedimentary inputs from the Tasmanian shelf. Southward advection of subtropical waters has also been observed to supply Fe and Mn enriched waters to the subantarctic zone (Sedwick et al. 2008; Bowie et al. 2009; Latour et al. 2021). To date, no studies have investigated Fe and Mn co-limitation in the Australian sector of the Southern Ocean. Additionally, to our knowledge, there has been no prior study of the seasonality of Mn or Fe-Mn (co-)limitation in any subantarctic region.

This study presents the results of three shipboard incubation experiments performed in subantarctic waters in the Australian sector of the Southern Ocean examining Fe-Mn co-limitation in austral spring, summer, and autumn. We expect that following wind-mixing in winter, both dissolved Fe (dFe) and dMn levels should be higher in surface waters during spring due to supply from deeper waters/subsurface maxima and external sources (e.g. about 0.3-0.4 nM for dFe and dMn; Bowie et al. 2009; Latour et al. 2021). Therefore, we hypothesize Fe and Mn will not (co-)limit phytoplankton growth in spring. In summer, dFe and dMn should decrease due to biological uptake and reduced vertical nutrient inputs resulting from stronger stratification. Hence, Fe limitation of phytoplankton growth will likely occur. Iron stress may increase phytoplankton Mn requirements (Peers and Price 2004), and due to the decrease of dMn concentrations from biological uptake during the spring season, dMn may (co-)limit phytoplankton growth. In autumn, trace metal levels should be at their lowest, hence we hypothesize Mn, Fe or both will strongly limit phytoplankton growth, depending on the ratios of both elements relative to biological demand.

Material and Methods

SAMPLING

The bioassay experiments were performed onboard the RV *Investigator* during three voyages, IN2018-V04 (September/October 2018, austral spring), IN2019-V02 (March/April 2019, austral autumn) and IN2020-V08 (December/January 2020-21, austral summer). The first experiment was conducted at Process Station 2 (PS2) of the East Australian Current voyage IN2018-V04 (45.44°S, 153.31°E) and the following two experiments at the Southern Ocean Time Series (SOTS) station (46.80°S, 141.884°E) (Figure 1). Both sites are within the subantarctic zone to the southeast and southwest of Tasmania, respectively (Bowie et al. 2011).

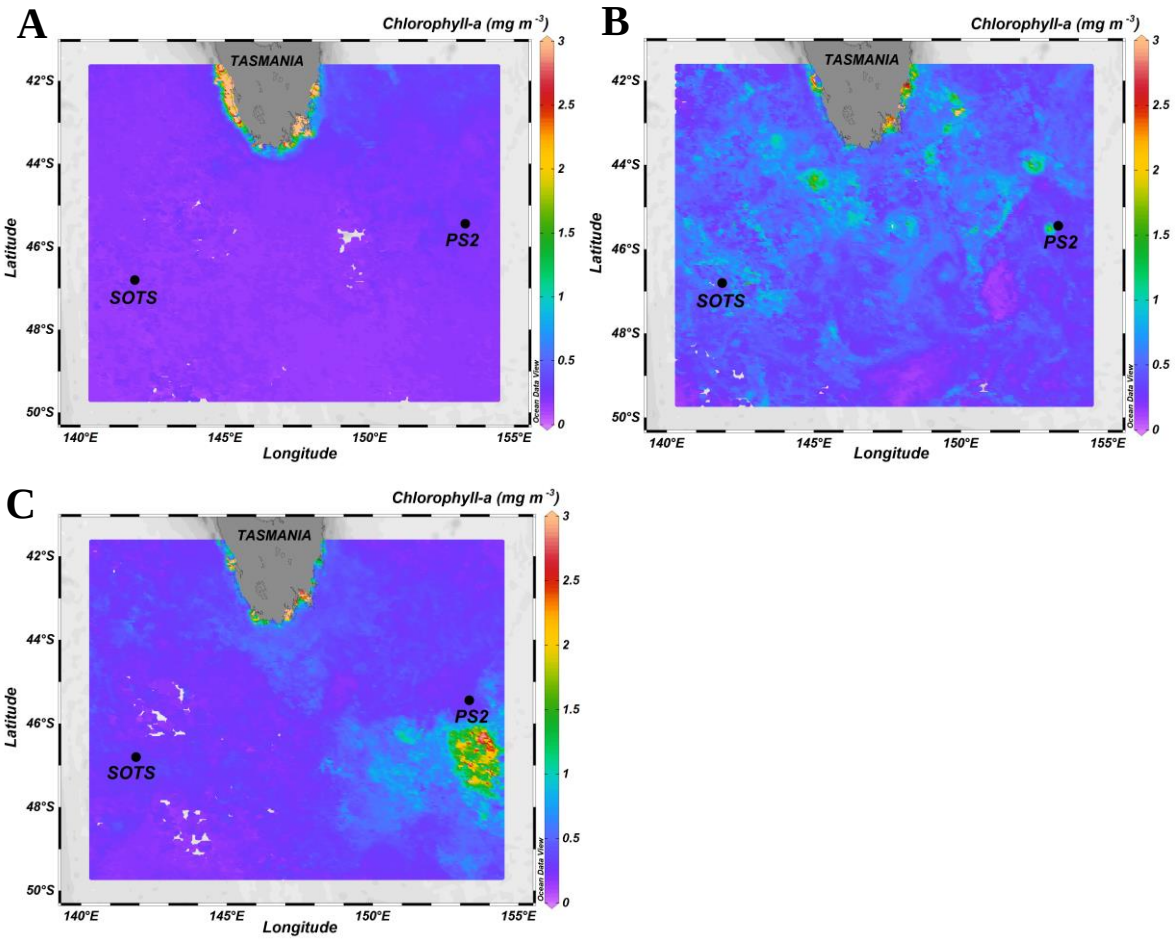

Figure 1: Sites sampled for each experiment. The background image colour shading represents the monthly average surface chlorophyll-a concentrations measured by satellite (MODIS-Aqua, 8-day average 4 km) for the month when each of the bioassay experiments was performed. A: phytoplankton incubations at PS2 during the spring voyage (IN2018-V04), monthly average for September 2018. B: phytoplankton incubations at SOTS during the summer voyage (IN2020-V08), monthly average for December 2020. C: phytoplankton incubations at SOTS during the autumn voyage (IN2019-V02), monthly average for March 2019.

Seawater used for the bioassay experiments was collected at 15 m depth for the first two experiments (spring and autumn) and at 20 m for the summer experiment using a polyurethane powder-coated aluminium rosette, or "Trace Metal Rosette" (TMR) (Sea-bird Scientific, USA; Holmes et al. 2020). Samples for macronutrients, flow cytometry and photophysiology analyses were collected from the

TMR to characterise the initial phytoplankton communities. Polycarbonate bottles used for the incubations were washed with Neutracon detergent for 48h, and then in 10% hydrochloric acid (HCl) for 7 days to remove trace metal contamination. After multiple Milli-Q water rinses, bottles were dried overnight in an ISO Class 5 laminar flow hood before being double-bagged in plastic. Onboard, the bottles were rinsed three times with the incubation seawater before filling them inside an ISO Class 5 containerized clean room. The seawater was unamended (Control) or spiked with a solution of Fe, Mn or a combination of both. The Fe and Mn spikes were prepared in 0.01 M Ultrapure HCl using ultrapure salts of $FeCl_3$ (or $FeNO_3$ for the spring experiment) and $MnCl_2$. Triplicates were used for each treatment, resulting in 12 bottles for 4 treatments, named hereafter: Control, +Fe, +Mn, and +FeMn. Concentrations of Fe and Mn were adjusted to reach a final concentration of at least 2 nM, which we considered as nutrient-replete conditions (Browning et al. 2021). The bottles were then incubated in deck board incubators inside mesh bags to reproduce the light penetrating the surface ocean, at approximately 15 m (80% of incident irradiance). Deck board incubators allowed the algal communities to follow their regular diel light:dark cycles. The temperature of the incubators was maintained by a continuous flow of seawater, keeping the bottles at the same temperature as the surrounding surface (~ 7 m) seawater. Sampling was done at day 7 for macronutrients, flow cytometry and photophysiology analyses for each experiment. Flow cytometry samples were fixed using 2% (v/v) glutaraldehyde (Electron-microscope grade, 25%), for phytoplankton samples collected during the second voyage in autumn 2019. For the summer 2020 voyage, a mixture of formaldehyde-hexamine (18%:10% v/w) was used to preserve phytoplankton samples. Due to a technical issue, flow cytometry samples from the spring 2018 voyage were lost and are therefore not presented in this study. All bacteria samples were fixed using 2% glutaraldehyde (Electron-microscope grade, 25%). All flow cytometry samples were held at 4°C in the dark for 25-30 min after being fixed and were then flash-frozen in liquid nitrogen and stored in a -80°C freezer until analyses back onshore.

Following the subsampling, a portion of the remaining seawater was dispensed into 300 mL acid-washed polycarbonate bottles and spiked with 16-20 µCi of Sodium ^{14}C-bicarbonate ($NaH^{14}CO_3$; specific activity 1.85 GBq mmol^{-1}; PerkinElmer, USA) and 0.2 nM of an acidified ^{55}Fe solution ($^{55}FeCl_3$ in 0.1 M Ultrapure HCl; specific activity 30 MBq mmol^{-1}; PerkinElmer; Ellwood et al. 2020). Bottles were then incubated in the deck board incubators for another 24 h, under the same conditions as the bioassay experiments. The spiked samples were then filtered sequentially through 0.2, 2 and 20 µm polycarbonate filters (47 mm diameter; Poretics, USA), separated by 200 µm nylon mesh spacers. The filters were washed with Titanium(III) EDTA – citrate reagent for 5 min to dissolve Fe (oxy)hydroxides and remove extracellular particle-bound ferric ions and rinsed three times with 15 mL of 0.2 µm-filtered seawater. Finally, filters were placed in 20 mL glass vials (Wheaton Industries, USA) and acidified with 200 µL of 1.2 M HCl. These filters were then stored at room temperature for analyses on shore.

ANALYSIS

Dissolved macronutrients were analysed onboard using segmented flow analysis (Rees et al. 2018). One silicic acid measurement was removed from the analysis due to an inconsistent result (autumn experiment, in the "Mn" treatment). In summer, several silicic acid concentrations measured had a value below the detection limit (0.2 µM) and were therefore replaced by this same value. Final nitrate concentrations are not presented due to the use of an $FeNO_3$ solution for the Fe spike during the spring experiment. However, initial nitrate concentrations are mentioned in the discussion. Phosphate and silicic acid uptake rates were calculated by subtracting the final value measured in each bottle from the initial concentrations to calculate an average uptake rate per week over the 7-day period of incubation. Initial dissolved trace metal concentrations were measured through Sector Field Inductively Coupled Plasma mass spectrometry (SF-ICP-MS) after preconcentration and matrix removal through seaFAST at the Australian National University (Canberra, Australia). Dissolved Fe and Mn concentrations were used to estimate Mn deficiency relative to Fe as $Mn^* = dMn\text{-}dFe/R_{Fe:Mn}$, where $R_{Fe:Mn}$ is the average Fe:Mn ratio of phytoplankton (Moore 2013; Browning et al. 2021). If $Mn^* > 0.1$, this suggests Mn replete conditions.

Fast Repetition Rate Fluorometry (FRRF) was used to determine the maximum photochemical efficiency (F_v/F_m) and functional absorption cross section (σ_{PSII}) of photosystem II (PSII) using a Light-induced Fluorescence Transients Fast Repetition Rate (LIFT-FRR) fluorometer (Soliense, USA). After low light (2 µmol photons m^{-2} s^{-1}) acclimation for ~30 minutes, samples were exposed to 140 flashes of light every 2.5 µsec (saturation sequence) to saturate PSII and the first stable electron acceptor, Q_A after which the time interval between flashes was increased exponentially (relaxation sequence) for 90 flashes. F_v/F_m (where $F_v = F_m - F_o$) was calculated from F_o and F_m, which refer to the minimum and maximum fluorescence in the dark-acclimated state, respectively. F_v/F_m and σ_{PSII} were determined from the mean of 200 iterations of the fluorescence induction and relaxation protocol measured at 470 nm. At least 10 acquisitions were measured for each sample and used to calculate the average value of F_v/F_m and σ_{PSII}. Due to recalibration of the instrument between voyages, no direct comparison of the initial fluorescence (F_o) results can be made between seasons, but only between treatments for the same season.

Flow cytometry samples were analysed at Menzies Institute for Medical Research (University of Tasmania, Hobart), using an Aurora Cytek flow cytometer. This instrument can measure particles ranging from 200 nm up to at least 60 µm. However, the largest size particles possibly measured by this instrument has not yet been determined. Briefly, frozen samples were thawed at 37°C for 5-10 minutes before running 500 µL of unstained samples at flow rates of ~50 µL per minute, using Milli-Q water as sheath fluid. Violet and blue excitation lights were used to differentiate main phytoplankton groups through their fluorescence pigments: chlorophyll with red fluorescence and phycoerythrin with orange fluorescence, respectively, against forward scatter (FSC). All scatter and fluorescence parameters were

analysed based on values from the integrated area of the excitation peak. Results obtained from both the summer and autumn voyages were analysed using SpectroFlo software. For an overall comparison between the two seasons, phytoplankton communities were divided into three gates: picoeukaryotes, nanoeukaryotes and large phytoplankton (microeukaryotes), identified on the violet channel (V12, 405 nm excitation, 692 nM emission) against FSC. If the signal from V12 was saturated, we used another excitation wavelengths (B7, 488 nm excitation, 661 nM emission). Picocyanobacteria were isolated on another fluorescence channel (B4, 488 nm excitation, 581 nM emission) due to the presence of phycoerythrin (Marie et al. 1999). Cell counts per unit volume were determined from the instrument through the known volume analysed. We then used the cell counts to calculate the relative importance of each group in terms of population size (*Fpop* described below) by comparing their size (FSC) and abundance, using the following equation from Bach et al. (2018):

$$Fpop = \frac{Npop \times FSCpop}{Nall \times FSCall} \quad (1)$$

Where F represent the fraction of size (size is here represented by the parameter FSC) produced by a specific population (pop). N represents an abundance via cell count of a specific population or all phytoplankton cells (all).

Heterotrophic bacterial counts were performed after the addition of SYBR Green I stain (1000-fold dilution) on thawed fixed samples. Samples were incubated with the stain for 15 minutes at room temperature in the dark. Then, a 50 µL aliquot of stained sample was run on the instrument at high flow rate. Bacteria were identified using blue excitation and green fluorescence (B2, 488 nm excitation, 525 nM emission). Cell counts were determined as described above for phytoplankton.

Iron uptake and net primary productivity (carbon uptake) were determined by measuring disintegrations per minute (DPM) on a liquid scintillation counter (PerkinElmer Tri-Carb 2910 TR). Filters were incubated at least 24h prior analysis in 10 mL of Ultima Gold liquid scintillation cocktail (Perkin Elmer). Daily carbon incorporation rates were estimated following Hoppe et al. (2017). The uptake of ^{55}Fe and ^{14}C were corrected for ambient dFe and dissolved inorganic carbon concentrations.

STATISTICAL TESTS

Statistical analyses were performed in R (R "stats" package; R Core Team 2020). Datasets were initially examined for homogeneity of variance using a Levene's test, and normality using a Shapiro-Wilk. Where data were both normally distributed and homoscedastic, significant differences between treatments were investigated using a one-way analysis of variance (ANOVA) with a Tukey's HSD post hoc test. Otherwise, a Kruskal-Wallis test was performed followed by a Wilcoxon signed-rank test where the former result was significant. A p-value of 0.05 was used to identify significant difference between treatments.

During the autumn experiment, no statistical tests could be performed on the Fe uptake results for the +Fe treatment due to a mistake in the radioisotope additions.

Results

INITIAL CONDITIONS

Oceanographic conditions differed between the three experiments across temperature, salinity and silicic acid profiles (Figure 2). In spring, the surface ocean was characterized by a deep mixed layer depth (MLD), down to 200 m. Temperature, salinity and silicic acid concentrations were constant within the mixed layer with values at about 10.5°C, 34.9 g kg^{-1} and < 3 µM, respectively. In summer, stronger stratification was observed with the MLD reaching just below 100 m. The surface temperature was like spring but lower below 25 m (about 10°C). In summer, the salinity was much lower than in spring (< 34.6 g kg^{-1}). Similarly, silicic acid concentrations were lower in summer, down to 1 µM in surface waters. In autumn, the MLD reached 100 m, where the temperature was ≥ 11°C and the salinity was like summer conditions. Silicic acid concentrations were the lowest, with less than 1 µM in surface waters.

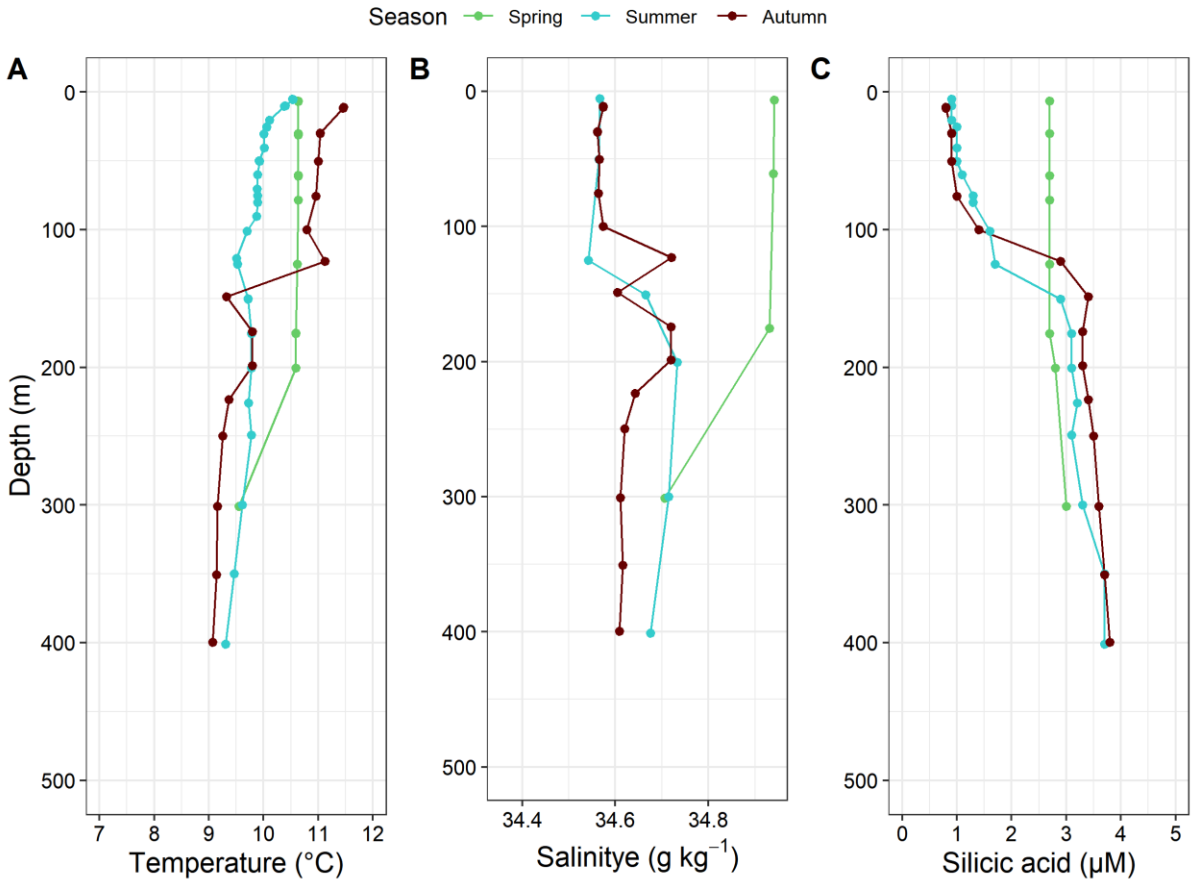

Figure 2: Temperature (A), salinity (B) and silicic acid concentrations (C) depth profiles measured at the experiment sites: PS2 (spring) and SOTS (summer and autumn). Colours represent the seasons: spring in green, summer in blue and autumn in brown.

Initial dFe and dMn concentrations present in the incubated seawater were slightly different between seasons (Table 1). The dFe concentration was the highest in summer, with intermediate values measured in spring and lowest concentrations in autumn. Similarly, the lowest dMn concentration was also recorded in autumn. However, both the spring and summer experiments had similar initial dMn concentrations. The calculated Mn* values were high (0.16-0.25) with the lowest Mn* observed in autumn (Table 1).

Table 1: Initial mean dFe and dMn concentrations with standard deviations measured in (or near) the seawater incubated for the three experiments and the calculated Mn* according to Browning et al. (2021): spring at PS2 in 2018 (n = 2), summer at SOTS in 2020 (n = 1) and autumn at SOTS in 2019 (n = 3). *Single measurements were performed for dFe and dMn in summer and dMn in autumn, in these cases the method error is indicated. In autumn, both dFe and dMn values came from a near cast.

Experiment	**Spring (PS2)**	**Summer (SOTS)**	**Autumn (SOTS)**
Depth of water collected (m)	15	20	15
dFe (nM)	0.31 ± 0.001	0.50 ± 0.03*	0.15 ± 0.04
dMn (nM)	0.37 ± 0.032	0.44 ± 0.03*	0.26 ± 0.03*
Mn*	0.25	0.25	0.16

MACRONUTRIENT DRAWDOWN

Both initial phosphate and silicic acid concentrations present in the seawater incubated for each experiment, along with the final concentrations measured after 7 days of incubations are presented in Figure 3. Focusing on the initial conditions, phosphate concentrations ranged from 0.71 to 0.82 µM, with the lowest value observed in autumn and the highest in spring. Similarly, the lowest initial silicic acid concentrations were observed in autumn (0.8 µM) and the highest in spring (2.8 µM).

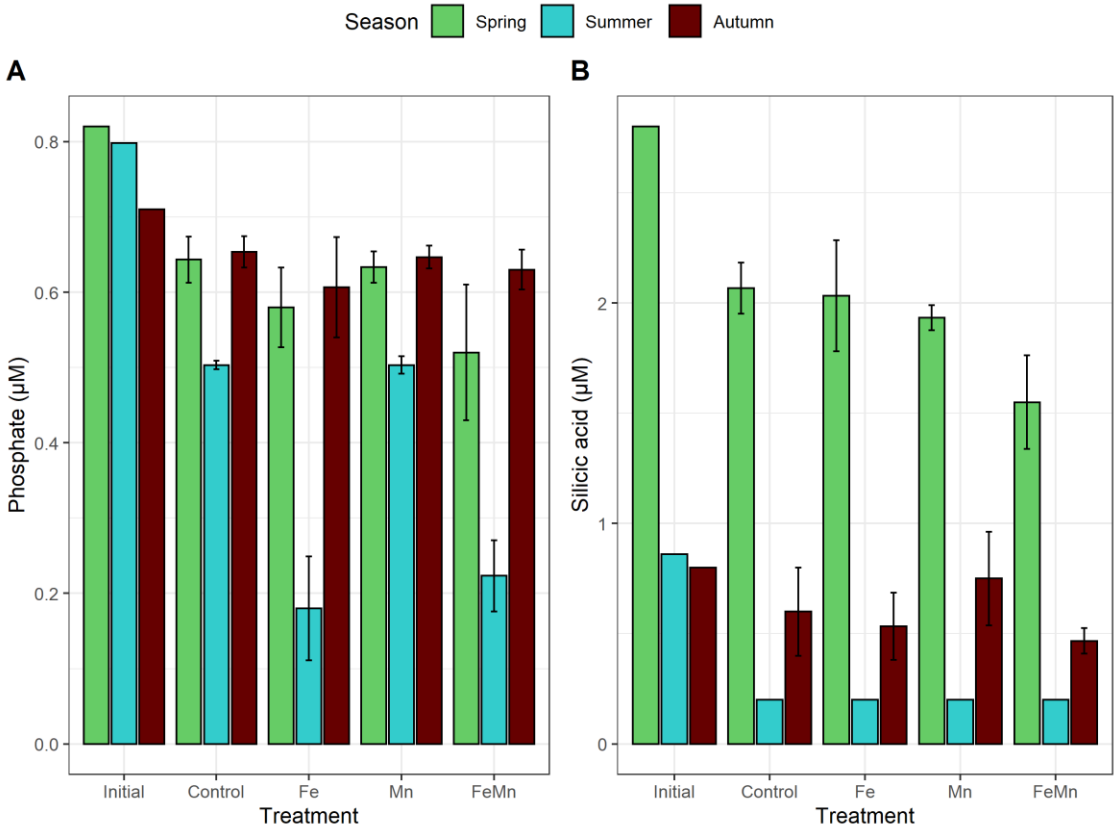

Figure 3: Phosphate (A) and silicic acid (B) concentrations (µM) measured in the initial water incubated ("Initial"), and after seven days of incubations for each treatment: Control ("Control"), +Fe ("Fe"), + Mn ("Mn"), +FeMn ("FeMn"). The colour represents the season of the experiment: green for spring, blue for summer and brown for autumn. Error bars represent the standard deviations and are smaller than the symbols when not visible (n = 3, except for the initial treatment where n = 1).

Phosphate and silicic acid concentrations decreased over the 7-day incubation, across all seasons and treatments. However, the uptake of both nutrients between each treatment varied seasonally. In spring, no significant differences were observed by day 7 in phosphate and silicic acid concentrations, between the control and the other treatments (ANOVA). In summer, we observed a significant decrease in phosphate concentrations only in the treatments where Fe was added (+Fe and +FeMn), compared to the control (*p-value* < *0.05*, Tukey's HSD). No significant drawdown of phosphate was observed in the Mn treatment, compared to the control. In summer, all treatments were characterized by final silicic acid concentrations below the detection limit (0.2 µM). In autumn, no significant differences were observed in either phosphate or silicic acid concentrations between treatments (ANOVA).

The uptake ratios for both phosphate and silicic acid differed seasonally (Table 2). In spring, no significant differences in phosphate and silicic acid uptake rate were observed between treatments (ANOVA). In summer, both Fe additions (+Fe and +FeMn) resulted in a very strong increase in the phosphate uptake rate, which doubled compared to the control and Mn treatments (*p-value* < *0.05*, Tukey's HSD). During this season, the treatment effects are impossible to interpret for the silicic acid uptake rates as concentrations were drawn down below the detection limit (0.2 µM) (Figure 3 and Table

2). In autumn, we did not observe any significant differences in the uptake rates for either phosphate or silicic acid between treatments (ANOVA).

Table 2: Average uptake rates of phosphate and silicic acid (µM week^{-1}) and standard deviations for each treatment calculated over the 7-day incubation period for each experiment (n=3). *In summer, all final silicic acid concentrations were below the detection limit (0.2 µM) and hence replaced with 0.2 µM. Consequently, the calculated uptake rate is identical in each treatment and cannot be interpreted.

	Treatment	**Control**	**+Fe**	**+Mn**	**+FeMn**
Phosphate	Spring	0.18 ± 0.03	0.24 ± 0.05	0.19 ± 0.02	0.30 ± 0.09
	Summer	0.04 ± 0.001	0.09 ± 0.01	0.04 ± 0.002	0.08 ± 0.01
	Autumn	0.06 ± 0.02	0.10 ± 0.07	0.06 ± 0.02	0.08 ± 0.03
Silicic acid	Spring	0.73 ± 0.12	0.77 ± 0.26	0.87 ± 0.06	1.25 ± 0.21
	Summer	0.66* ± NA	0.66* ± NA	0.66* ± NA	0.66* ± NA
	Autumn	0.20 ± 0.20	0.27 ± 0.15	0.05 ± 0.20	0.33 ± 0.06

PHOTOPHYSIOLOGY

The photochemical efficiency of PSII (F_v/F_m) differed between treatments and seasons (Figure 4A). In spring, no significant differences in final F_v/F_m values were measured between treatments (ANOVA). In summer, only the treatments with Fe additions (+Fe and +FeMn) maintained F_v/F_m values as high as the initial community, and significantly higher than the control and +Mn treatments (*p-value* < *0.05*, Tukey's HSD). In autumn, we measured significantly higher F_v/F_m values in both treatments with Fe additions (+Fe and +FeMn) compared to the +Mn treatment (*p-value* < *0.05*, Tukey's HSD). However, F_v/F_m values measured in both Fe treatments were not significantly higher than the control (ANOVA).

The functional absorption cross section of PSII (σ_{PSII}) differed between seasons (Figure 4B). The initial value was higher in summer compared to spring and autumn. In spring, we observed a significant decrease in σ_{PSII} only in the +FeMn treatment, compared to the other treatments (*p-value* < *0.05*, Tukey's HSD). In summer, both treatments with Fe additions (+Fe and +FeMn) were characterized by a decrease in σ_{PSII} compared to the control and +Mn treatments (*p-value* < *0.05*, Tukey's HSD). In autumn, no significant differences in σ_{PSII} were observed between treatments (ANOVA).

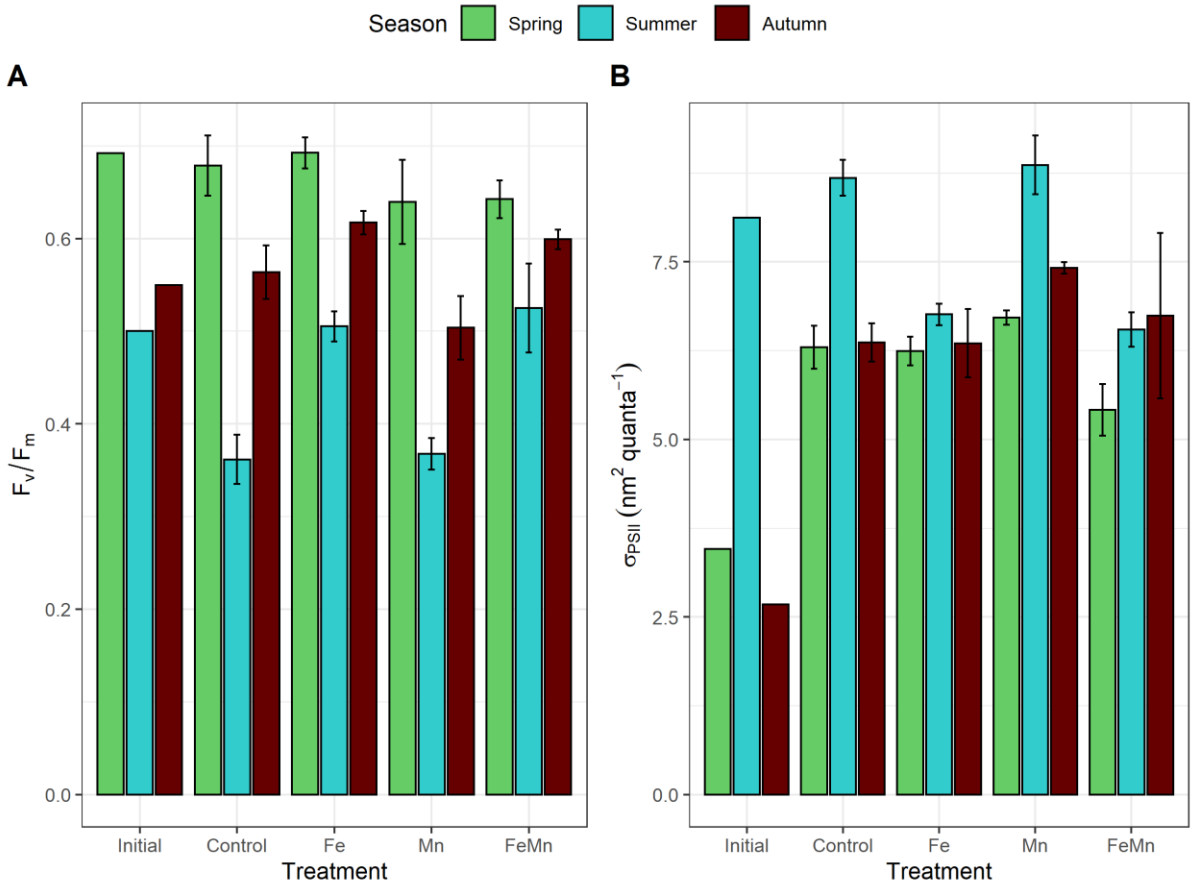

Figure 4: A) Photochemical efficiency of photosystem II (F_v/F_m) and B) functional absorption cross section of PSII (σ_{PSII}) in nm^2 $quanta^{-1}$, measured for the initial algal communities incubated ("Initial") and after 7 days of incubation, in each treatment: Control, +Fe ("Fe"), + Mn ("Mn"), +FeMn ("FeMn"). The three colours show the different seasons: green for spring, blue for summer and brown for autumn. Error bars represent the standard deviations (n = 3, except for the initial treatment where n = 1).

FLOW CYTOMETRY

Notable differences in phytoplankton community composition were observed between summer and autumn. In summer, picoeukaryotes dominated the cell counts (Table 3). However, nanoeukaryotes dominated community population size, as defined by equation (1) in the method section (Figure 5A). In autumn, cyanobacteria dominated the counts (Table 3) while nanoeukaryotes dominated the community population size (Figure 5B).

Table 3: Counts of phytoplankton cell (cell mL^{-1}) measured in the main gated populations: picoeukaryotes ("Picoeuk."), cyanobacteria ("Cyano."), nanoeukaryotes ("Nanos."), large phytoplankton ("Large phyto.") and bacteria for the summer and autumn experiments, in each treatment. The mean value along with the standard deviation (n=3) is presented.

Summer					
Treatment	*Picoeuk.*	*Cyano.*	*Nanos.*	*Large phyto.*	*Bacteria*
Initial	10880	4150	5630	130	620400
Control	4820 ± 683	5517 ± 1142	15540 ± 560	213 ± 32	379703 ± 92672
Fe	4847 ± 3032	4980 ± 1802	21070 ± 2208	650 ± 191	401147 ± 32324

Mn	5203 ± 942	5883 ± 924	12430 ± 1311	170 ± 36	410350 ± 29142
FeMn	6317 ± 3163	5967 ± 1438	25593 ± 12130	593 ± 15	388403 ± 79888
			Autumn		
Treatment	*Pico.*	*Cyano.*	*Nano.*	*Large phyto.*	*Bacteria*
Initial	22230	25240	2260	80	655040
Control	12733 ± 3958	18743 ± 5479	4473 ± 2789	67 ± 21	734727 ± 123795
Fe	14220 ± 9869	27023 ± 2675	4230 ± 1897	77 ± 15	1080060 ± 764544
Mn	23865 ± 460	65405 ± 30823	4800 ± 891	55 ± 35	1280305 ± 323593
FeMn	12830 ± 1193	29450 ± 16046	4987 ± 876	117 ± 32	940517 ± 219637

After 7 days of incubation, no significant difference in cell counts were observed between treatments across seasons (ANOVA), but some small changes occurred in the sized-based metric. In autumn, the addition of Mn led to an increase in the cyanobacteria population size relative to the whole phytoplankton community (*p-value* < *0.05*, Tukey's HSD). This change was not observed during the summer experiment.

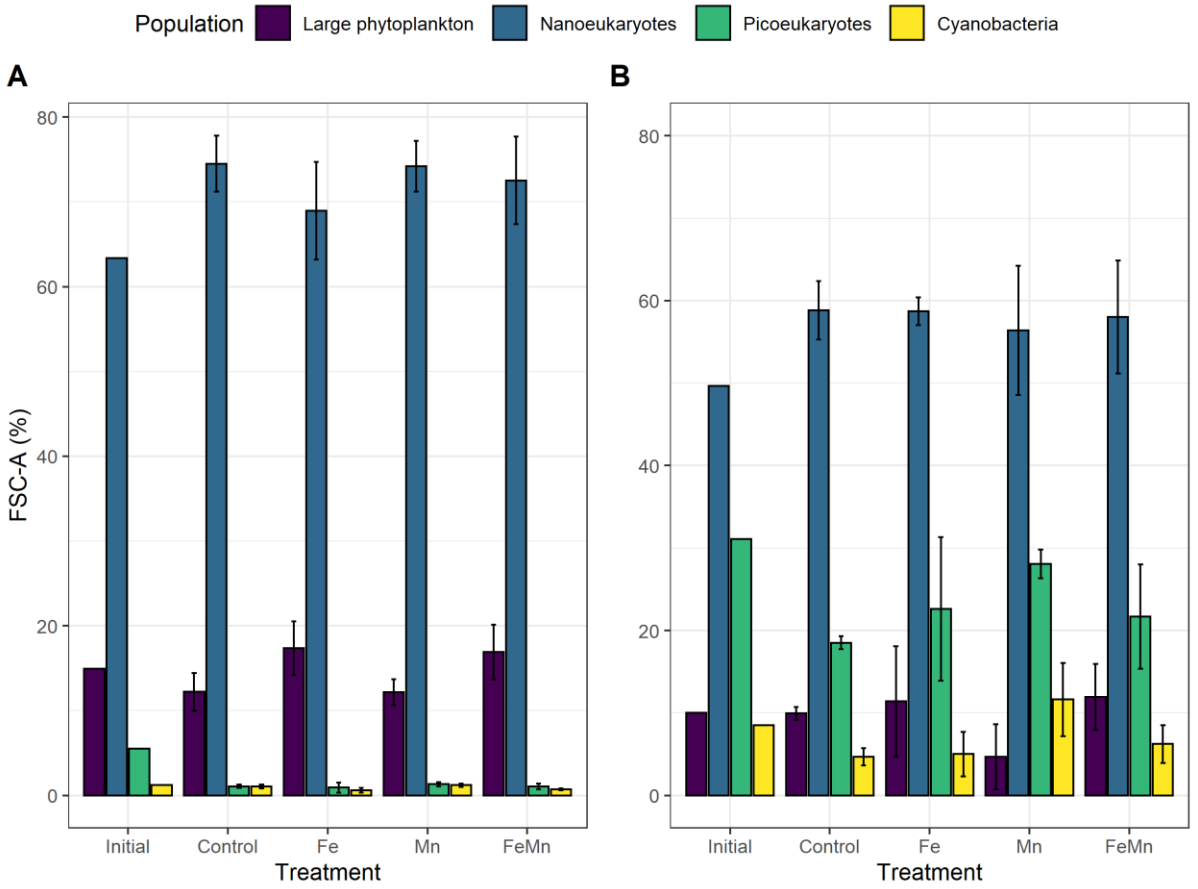

Figure 5: Relative contribution of four gated populations compared to all phytoplankton cells: large phytoplankton (microeukaryotes), nanoeukaryotes, picoeukaryotes and cyanobacteria in terms of population size (FSC), as defined in equation (1) for summer (A) and autumn (B). These values were calculated according to the equation of Bach et al. (2018). Error bars represent the standard deviations (n = 3, except for the initial treatment where n = 1).

IRON AND CARBON UPTAKE

Different rates of Fe uptake were observed between seasons and size fractions (Figure 6). Focusing on the 0.2-2 µm size fraction, no significant differences were observed between treatments across seasons. However, in summer and autumn, Fe uptake rates increased under Fe additions, with higher average values in the +Fe addition alone. The highest Fe uptake was observed in autumn (396.8 ± 169 pM d^{-1}), whereas mean Fe uptake was lower when both Fe and Mn were added (174.6 ± 27 pM d^{-1}). No significative difference was observed between treatments in autumn, likely resulting from a small dataset (only 2 data points for the +Fe treatment).

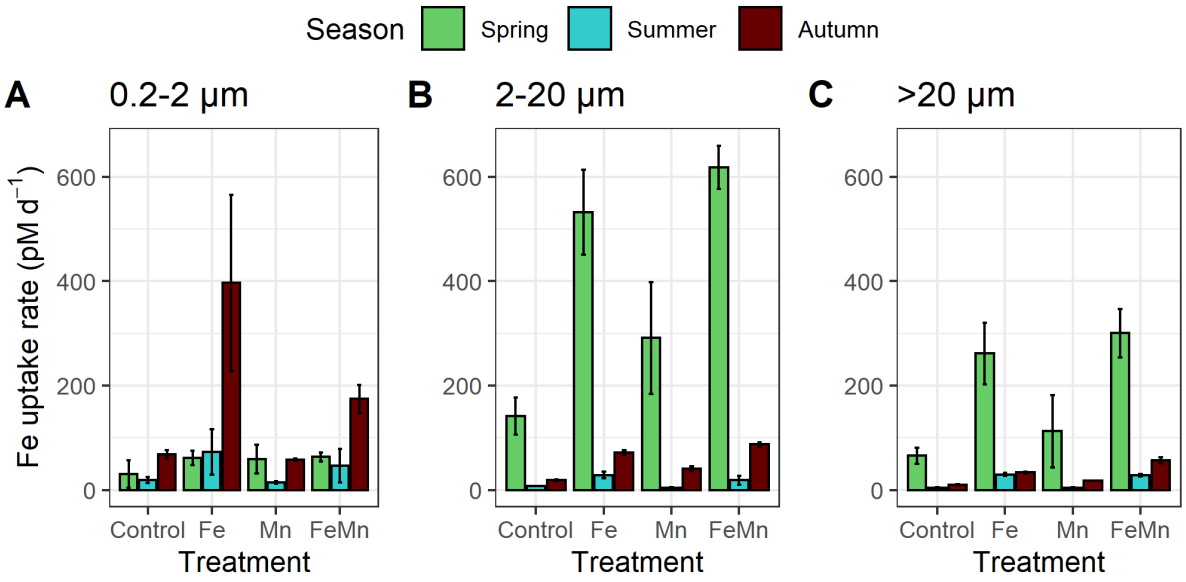

Figure 6: Fe uptake (pM d^{-1}) measured in each size fraction and for the three seasons: spring in green, summer in blue and autumn in brown. During the autumn experiment, only two datapoints were recorded for the +Fe treatment. Error bars represent the standard deviations and are smaller than the symbols when not visible (n = 3).

In the 2-20 µm size class (Figure 6B), Fe uptake was highest in spring with significantly higher Fe uptake under both Fe additions compared to the control and +Mn treatments (*p-value* < *0.05*, Tukey's HSD). The +Mn treatment induced an increase in Fe uptake. However, it was not significantly higher than the control. In comparison, both summer and autumn seasons were characterized by much lower Fe uptake in the 2-20 µm size fraction. In summer, Fe uptake rates were significantly higher than the control only in the +Fe treatment, with a mean value four times higher than Fe uptake in the control (*p-value* < *0.05*, Tukey's HSD). The combined +FeMn addition did not result in a significant stimulation of Fe uptake compared to the control (*p-value* = *0.06*, Tukey's HSD). In autumn, no significant differences in Fe uptake were observed between treatments (Kruskal-Wallis test).

The >20 µm size class (Figure 6C) was also characterized by higher Fe uptake values measured in the spring. In both spring and summer, Fe uptake was significantly higher in both treatments with Fe additions (+Fe and +FeMn), compared to the control and +Mn treatments (*p-value* < *0.05*, Tukey's

HSD). In autumn, no significant differences in Fe uptake were observed between treatments, which could result from a low number of data points (Kruskal-Wallis test).

Net primary productivity, measured through carbon uptake, also strongly varied between seasons and size fractions (Figure 7). In spring, no significant difference in carbon uptake rates were observed between treatments in the small size fraction (ANOVA). In summer, we measured the highest carbon uptake for picoeukaryotes in the +Fe treatment compared to the control (*p-value* < *0.05*, Tukey's HSD). In addition, both Fe treatments (+Fe and +FeMn) had significantly higher carbon uptake rates than the +Mn treatment (*p-value* < *0.05*, Tukey's HSD). In autumn, no significant differences in carbon uptake were observed in the 0.2-2 µm size class (Kruskal-Wallis test).

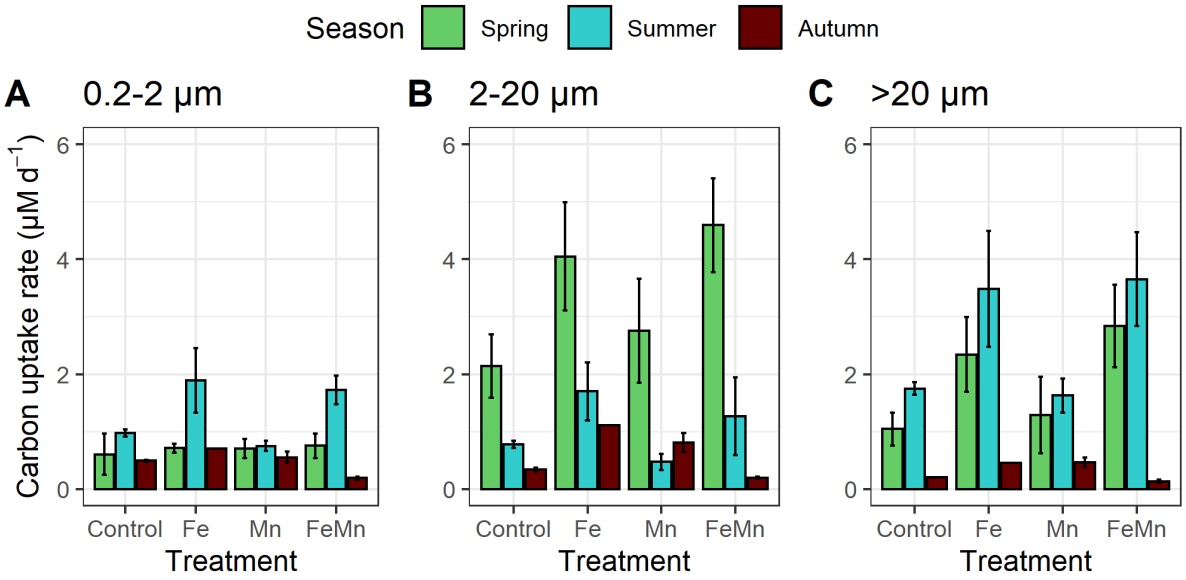

Figure 7: Carbon uptake (µM d^{-1}) measured in each size fraction and for the three seasons: spring in green, summer in blue and autumn in brown. Due to a manipulation mistake during the autumn experiment, only one datapoint was recorded for the +Fe treatment. For the other treatments, error bars represent the standard deviations and are smaller than the symbols when not visible (n = 3).

For the nanoeukaryotes (2-20 µm) during the spring season, only the +FeMn treatment had higher carbon uptake rates than the control (*p-value* < *0.05*, Tukey's HSD). In summer, a significant difference between carbon uptake was only observed between the +Fe and +Mn treatments (*p-value* < *0.05*, Tukey's HSD), with higher carbon uptake with Fe addition alone. In autumn, no significant differences were observed between treatments (Kruskal-Wallis test).

In the >20 µm size class, there was no significant difference in carbon uptake between treatments in spring (Kruskal-Wallis test). In summer, carbon uptake was only significantly higher in the +FeMn treatment compared to the control treatment (*p-value* < *0.05*, Tukey's HSD). The carbon uptake rates measured in the +Fe treatment, while elevated, were not significantly different than the control (*p-value* = *0.05*, Tukey's HSD). However, both +Fe and +FeMn treatments had a higher carbon uptake than in

the +Mn treatment (*p-value* < *0.05*, Tukey's HSD). In autumn, no significant differences were observed in the carbon uptake between treatments within this size class (Kruskal-Wallis test).

Iron to carbon (Fe:C) uptake ratios differed between seasons and treatments, with overall higher ratios measured in autumn (Figure 8). Across all sizes, Fe:C ratio ranged between 33 to 153 µmol mol^{-1} in spring, 1 to 18 µmol mol^{-1} in summer and from 34 to 915 µmol mol^{-1} in autumn. In the 0.2-2 µm size fraction, no significant differences were observed between treatments across seasons (ANOVA for spring and summer; and Kruskal-Wallis test for autumn).

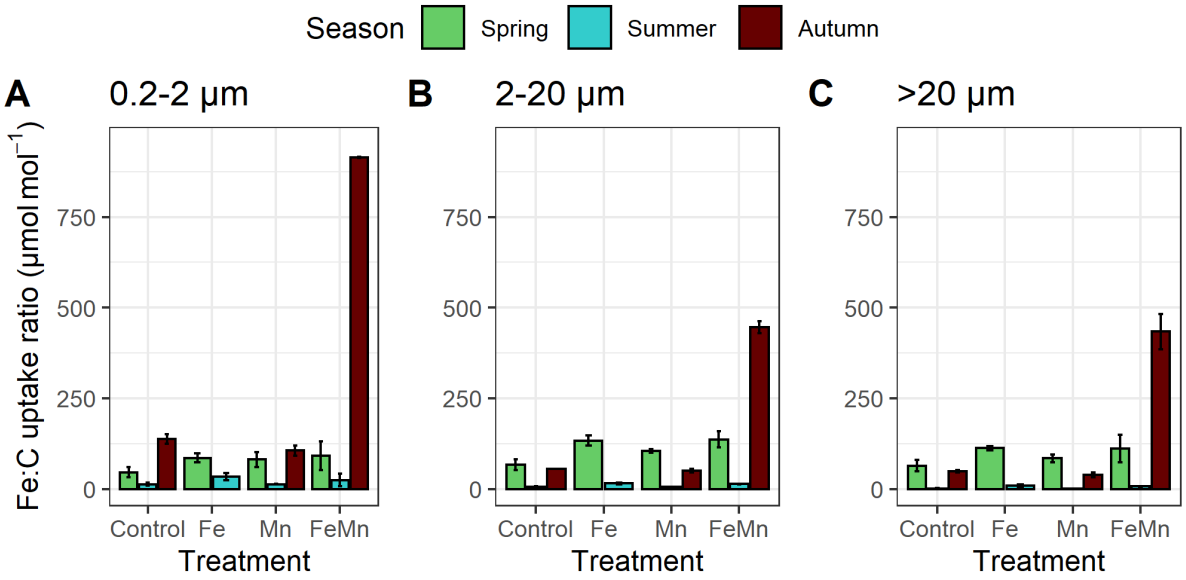

Figure 8: Iron to carbon (Fe:C) uptake ratio (µmol mol^{-1}) measured in each size fraction and for the three seasons: spring in green, summer in blue and autumn in brown. The Fe:C ratio from the +Fe treatment in autumn was not included due to missing data. Error bars represent the standard deviations and are smaller than the symbols when not visible (n = 3).

For the nanoeukaryotes (2-20 µm), spring Fe:C uptake ratios were higher in +Fe and +FeMn treatments compared to the control treatment (*p-value* < *0.05*, Tukey's HSD). In summer, Fe:C ratios measured in +Fe and +FeMn treatments were higher than ratios measured in both the control and +Mn treatments (*p-value* < *0.05*, Tukey's HSD). In autumn, no significant differences were observed, likely resulting from a small dataset (Kruskal-Wallis test).

No significant differences in Fe:C uptake ratios for the microeukaryotes (>20 µm) were observed during the spring experiment (ANOVA), while Fe:C ratios were higher under +Fe and +FeMn compared to the control and +Mn treatments in summer (*p-value* < *0.05*, Tukey's HSD). In autumn, no significant differences were observed but again, this may result from a small dataset (Kruskal-Wallis test).

Discussion

CONTRASTING HYDROGRAPHIC SITES

Contrasting results may be expected between experiments due to the different locations of the spring experiment, done at PS2, and the two other experiments (summer and autumn), performed at SOTS. The intrusion of warmer and saltier waters from the subtropical zone are commonly observed in the northern part of the subantarctic zone near SOTS and can originate from either the mixing with waters from the Zeehan Current or mixing with waters and eddies from the East Australian Current (Bowie et al. 2011). In this study, the PS2 station, located southeast of Tasmania, is much more likely to be influenced by the East Australian Current, compared to the SOTS site. This explains the strong difference in salinity observed in the spring experiment compared to the two other experiments. However, autonomous seasonal records of phytoplankton communities from the SOTS station revealed no change in community composition due to the input of subtropical waters in the subantarctic zone (Eriksen et al. 2018). Hence, we suggest that the results of the three experiments are comparable, despite the influence of subtropical waters at PS2 in the spring experiment.

The three experiments undertaken were characterized by different initial macronutrient concentrations. Higher phosphate and silicic acid concentrations were observed at the beginning of the spring experiment, which is a characteristic of the early season following winter mixing of surface waters (Rintoul and Trull 2001). In contrast, macronutrient concentrations were lowest in autumn. Phosphate concentrations decrease during the summer season due to biological uptake but are expected to remain higher than limiting levels (Rintoul and Trull 2001). On the other hand, silicic acid concentrations decrease during the growth season, due to consumption from silicifying phytoplankton such as diatoms, silicoflagellates and radiolarians (Deppeler and Davidson 2017; Eriksen et al. 2018). In autumn, silicic acid concentrations reached limiting levels, down to 0.8 µM (Paasche 1973; Hutchins et al. 2001; Westwood et al. 2011). Therefore, silicic acid growth limitation of silicifying organisms may be expected during the autumn experiment. Nitrate concentrations are not presented here but initial levels were not considered limiting (nitrate + nitrite: 11.0 µm in spring, 10.2 µm in summer, 8.3 µm in autumn).

Initial trace metal concentrations were highest in spring for dMn and summer for dFe. It is surprising to observe higher summer dFe concentrations compared to the spring experiment. Usually, higher dissolved concentrations are recorded in the early season, resulting from i) aerosol depositions coming from proximal land (Perron et al. 2020), ii) southern advection of Fe and Mn enriched subtropical waters from the East Australian Current (Sedwick, et al. 2008; Bowie et al. 2009) and/or iii) replete trace metal levels present after the winter season associated with wind-mixing (Bowie et al. 2009). At the SOTS site, higher dFe concentrations observed in summer may result from entrainment following wind-

mixing events while decreasing autumn concentrations for both elements likely result from biological consumption.

Initial phytoplankton biomass in summer and autumn was dominated by pico- and nanoplankton, as previously observed in this subantarctic region (Fourquez et al. 2020). In summer, picoeukaryotes dominated phytoplankton abundance while picocyanobacteria were relatively important in autumn (Figure 5). It is likely that *Synechococcus* sp. dominated the picocyanobacteria, as has been previously observed at SOTS (Cassar et al. 2015; Fourquez et al. 2020). In all seasons, *in-situ* light limitation of phytoplankton growth is expected due to the deep mixed layer depths present (Figure 2). Indeed, Rintoul and Trull (2001) previously observed that a mixed layer depth of 75 to 100 m was deep enough to light limit phytoplankton growth in this region. Here, the mixed layer depth was at or ≥100 m (Figure 2). Initial physiological measurements indicated that the bulk phytoplankton communities were relatively healthy (F_v/F_m > 0.5) at all seasons (Figure 4). However, our data indicated various degrees of Fe limitation.

SEASONALITY OF IRON LIMITATION

Phytoplankton growth in subantarctic waters is usually assumed to be Fe limited (Boyd et al. 1999; Sedwick et al. 1999; Hutchins et al. 2001; Petrou et al. 2011). However, our experiments demonstrate that the degree of Fe limitation is seasonal. A previous review suggested Fe may limit subantarctic phytoplankton communities in spring (Boyd 2002). Contrasting with this hypothesis, no clear evidence of Fe stress was observed in our spring experiment. This may result from relatively elevated dFe concentrations in the early season, sufficient to maintain optimal phytoplankton growth at that time. This was supported by the high F_v/F_m values measured in all treatments (Figure 4A), suggesting efficient light utilization in PSII (Greene et al. 1992; Hopkinson and Barbeau 2008). Unfortunately, the lack of flow cytometry data for this season means that the initial composition of the phytoplankton community and how it evolved with Fe and Mn additions were not assessed. Previous reports showed this subantarctic region is characterized by a succession from large diatoms in spring toward weakly silicified diatoms in summer/autumn (Eriksen et al. 2018). From our Fe and carbon uptake results, it was observed that most of the Fe and carbon uptake came from nano- and microplankton in spring (Figure 6 and 7). Hence, it is possible the spring experiment took place during the transition from large diatoms (> 20 µm) toward smaller (2-20 µm) and more weakly silicified diatoms in response to decreasing ambient dFe and silicic acid concentrations (Eriksen et al. 2018).

The strongest signal of Fe limitation was observed during the summer experiment as highlighted by i) the drawdown of phosphate concentrations in both treatments where Fe was added (Figure 3A), and ii) the increase F_v/F_m and the decrease in σ_{PSII} with Fe additions (Figure 4). These results suggest that the addition of Fe alleviated phytoplankton stress (Greene et al. 1992; Petrou et al. 2011) and agreed with previous suggestion of dominant Fe limitation in summer (Boyd 2002). Although nitrate levels were

greatly drawn down by the end of the experiment within both Fe treatments (between 0.6 to 2 µM in 5 replicate bottles, and down to < detection limit levels in 1 replicate bottle), co-limitation from Fe and silicic acid may more likely occur toward the end of the experiment due to ongoing nutrient consumption (Figure 3B). Flow cytometry results indicated that nanoeukaryotes dominated the initial population size and remained the dominant group throughout the experiment in all treatments (Figure 5A). Combined with the high uptake of silicic acid observed in summer (Figure 3B), these results suggest the growth stimulation of relatively small diatoms, within the nanoeukaryote size range, in agreement with previous results (Eriksen et al. 2018). Despite an overall dominance of smaller diatoms, large phytoplankton (>20 µm) dominated primary productivity (Figure 7C). Microeukaryotes comprised about 15% of the population size (Figure 5) and may be composed of large diatoms and large dinoflagellates, as previously observed in subantarctic waters (Cassar et al. 2015; Eriksen et al. 2018). Coincident with this relatively high carbon uptake, very low Fe uptake rates were measured in both the nano- and micro- size classes, which suggest that these large summer phytoplankton species, likely diatoms, have low cellular Fe requirements (Strzepek et al. 2011; Gao et al. 2021). This assertion was supported by the very low Fe:C uptake ratios observed during summer in all size classes (Figure 8), implying that diatoms were able to sustain growth and substantial carbon assimilation with very low Fe requirements. Similarly, it is notable that the 0.2-2 µm size class had carbon uptake rates as high as the 2-20 µm size fraction, implying a similar efficiency in assimilating carbon between both size classes (Figure 7). However, relatively higher Fe uptake rates observed in the 0.2-2 µm size class may indicate higher efficiency in Fe uptake, possibly due to their lower surface area volume ratio (Sunda and Huntsman 1995; Strzepek et al. 2011). Notably, this size fraction also includes Fe uptake by heterotrophic bacteria but their contribution to Fe uptake was not determined.

In autumn, Fe limitation was evident, supported by the increase in F_v/F_m with Fe addition (Figure 4; +Fe treatment only) but to a lesser extent than in summer. In contrast to the summer experiment, phosphate and silicic acid drawdown remained much lower in autumn (Table 2), indicating that a factor other than Fe may be (co-)limiting phytoplankton growth. Given the low initial silicic acid levels observed (0.8 µM), silicic acid may be the primary variable limiting the growth of silicified organisms (Hutchins et al. 2001; Eriksen et al. 2018) and not dFe concentrations or other macronutrients considering phosphate (0.71 µM) and nitrate + nitrite levels (8.3 µM) remained above limiting levels (Sedwick et al. 1999; Rintoul and Trull 2001). However, the possibility of Fe and silicic acid co-limitation of diatoms growth cannot be excluded (Boyd 2002). A previous study in the subantarctic zone suggested a seasonal succession of limiting variables, with both Fe and silicic acid concentrations limiting the growth of heavily silicified diatoms in late summer and autumn, leading to a community shift toward non-silicified and/or lightly silicified diatoms with low Fe requirements (Hutchins et al. 2001). Relatively high Fe uptake rates were measured in all size classes during the autumn experiment compared to summer (Figure 6), possibly due to an upregulation of Fe acquisition in response to chronic

Fe limitation in these late season phytoplankton communities. In the >20 µm size class, it is possible dinoflagellates dominated phytoplankton abundance as silicic acid levels were likely limiting the growth of large diatoms (Eriksen et al. 2018). Unfortunately, we cannot confirm the phytoplankton community composition of the medium and small size class as additional information would be necessary, such as pigments analyses or microscopy. Flow cytometry did allow the identification of picocyanobacteria, which represented an important group during this season.

In autumn, picocyanobacteria, most likely *Synechococcus* sp. (Cassar et al. 2015) numerically dominated the phytoplankton community (Table 3). Previous flow cytometric analyses showed picocyanobacteria are a significant group within the subantarctic phytoplankton community, contributing about 20% to total phytoplankton biomass in mid-late summer (Cassar et al. 2015). In autumn, the contribution of picocyanobacteria to the population size doubled with +Mn addition (Figure 5). The photophysiology of picocyanobacteria differs from diatoms and other major phytoplankton groups (Suggett et al. 2009). This is mostly due to their use of phycobilisomes as light-harvesting pigments which results in lower maximum PSII photochemical efficiency (Suggett et al. 2004). Previous studies reported F_v/F_m values ranging from 0.1 to 0.6 for picocyanobacteria (Campbell et al. 1998; Koblıžek et al. 2001; Suggett et al. 2009). Hence, it is not straight-forward to link relatively low F_v/F_m values with Fe limitation within a phytoplankton community dominated by cyanobacteria. The increase in F_v/F_m observed in the +Fe treatment (Figure 4A) may indicate that a different population with an intrinsically higher F_v/F_m responded to Fe addition. The slightly higher silicic acid uptake rates observed with Fe additions (Table 2) suggest the growth of silicified organisms, possibly weakly silicified diatoms in this late season. However, it was previously shown that picocyanobacteria can accumulate silicon intracellularly as a hydrated siliceous network, associated with magnesium or calcium (Ohnemus et al. 2018). Hence, the higher silicic acid uptake may have also resulted from picocyanobacteria stimulation. These results highlight the complexity of identifying nutrient stress conditions from a bulk phytoplankton community dataset, where signals from specific taxonomic groups can get easily lost (Suggett et al. 2009). However, our findings provide evidence for a strong seasonality of Fe limitation and a seasonal succession of various phytoplankton groups, associated with their responses to key environmental constraints, particularly dFe and silicic acid concentrations (Eriksen et al. 2018). In addition, seasonality in phytoplankton responses to Mn additions were also observed.

EVIDENCE OF IRON-MANGANESE CO-LIMITATION

Overall, these seasonal experiments did not show a clear signal of Fe-Mn co-limitation, in comparison to the strong responses observed from Fe additions. This outcome concurred with the high Mn* values calculated for the three seasons (Table 1), fitting within the range of Browning et al. (2021) (0.16 -0.31 nM) for which Fe was limiting but not Mn. However, we observed some interesting responses to Mn addition, particularly from picocyanobacteria. In autumn, the addition of Mn noticeably stimulated the

550 growth of picocyanobacteria (Figure 5). The lower bulk F_v/F_m value observed in this treatment may
551 support the hypothesis of a dominant contribution from cyanobacteria, which often have an intrinsically
552 lower F_v/F_m than eukaryotic algae (Campbell et al. 1998; Koblıžek et al. 2001; Suggett et al. 2009). The
553 stimulation of the picocyanobacterial population under Mn addition may indicate that Mn was limiting
554 cyanobacterial growth. However, the F_v/F_m parameter is not a reliable indicator of PSII efficiency in
555 cyanobacteria as they have more flexible electron transport systems (Campbell et al. 1998) and PSII is
556 poorly excited by the wavelength (470 nm) used in this study. Cyanobacterial Mn requirements are still
557 poorly understood. Previous laboratory studies of *Synechocystis* (a freshwater cyanobacteria) showed
558 that dMn concentrations ≤ 100 nM reduces oxygen evolution capacity and results in the accumulation
559 of partially assembled PSII systems, and changes in the organization of photosystem I complexes
560 (Salomon and Keren 2011). In their most limiting Mn treatment, Salomon and Keren (2011) measured
561 a background dMn concentration of 1.8 nM, which is still much higher than what is commonly observed
562 in Southern Ocean open waters. However, oceanic strains may have adapted to lower surrounding dMn
563 concentrations by lowering their Mn requirements. This was previously shown in cyanobacteria
564 regarding adaptation to Fe limitation (Ferreira and Straus 1994). Twining et al. (2010) reported Mn cell
565 quotas (normalised to phosphate) ranging from 0.46 to 0.81 mmol/mol in *Synechococcus* sp. cells from
566 the Sargasso Sea, with strong variations between cyclonic/anticyclonic eddies and mode waters. In Fe-
567 limited Southern Ocean waters, for which there are no data on cyanobacteria, much lower Mn to
568 phosphate ratios were measured in autotrophic flagellates and, unlike diatoms, the ratio increased once
569 Fe stress was alleviated (Twining et al. 2004). Overall, there is insufficient information on the Mn
570 requirements of subantarctic cyanobacterial strains to predict the dMn concentrations at which they
571 become limited. However, our results provide the first evidence that Mn may limit cyanobacteria growth
572 in autumn, when small picoplankton dominate the biomass and surrounding dMn concentrations are
573 lowest. This implies Mn may be linked to deep carbon export as cyanobacteria have been observed to
574 significantly contribute to downward carbon export in subantarctic waters through aggregation (Waite
575 et al. 2000; Cassar et al. 2015) which increases their sinking rate (Jackson 2005). Hence, there may be
576 seasonality in the importance of Mn in stimulating phytoplankton growth, associated with specific
577 phytoplankton taxa such as cyanobacteria.

578 Another interesting result associated with Mn additions was the significant stimulation of carbon uptake
579 within the 2-20 µm size class in spring and within the >20 µm size class in summer, only occurring
580 under combined Fe and Mn additions (Figure 7). Increased carbon fixation and hence, photosynthesis,
581 suggest that these size classes of the phytoplankton community benefited from the combined addition
582 and may be Fe-Mn co-limited. Phytoplankton Mn requirements are directly linked to photosynthesis by
583 two processes: i) the number of PSII reaction centres, due to the central role of Mn in the oxygen-
584 evolving complex of PSII (Armstrong 2008) and, ii) the need for Mn to produce the superoxide
585 dismutase enzyme, to detoxify the cell of superoxide produced during photosynthesis (Peers and Price

2004; Wolfe-Simon et al. 2006). Increased Mn requirements were previously observed in Fe-limited diatoms, due to additional ROS production associated with Fe limitation (Peers and Price 2004). Hence, stimulation of carbon uptake observed under combined Fe and Mn additions during the summer experiment may be linked to ROS production and increased Mn requirement, knowing that phytoplankton communities were strongly Fe-limited (see previous section). Conversely, stimulation of carbon fixation measured under combined addition in spring is surprising considering phytoplankton communities were not Fe-limited. Instead, this enhanced carbon fixation may result from higher Mn demands associated with higher Fe requirements observed in these early phytoplankton communities.

Our results support the hypothesis that Mn concentrations may be low enough to limit the growth of a subset of the primary producers in this subantarctic region and hence to influence phytoplankton community composition. However, these effects appear to vary seasonally, and are subtle. Here, the evaluation of primary productivity through size-fractionated carbon uptake measurements coupled with flow cytometry helped us to identify these co-limitation signals but this approach is not commonly used. This highlights the need to use a combination of existing techniques, and to develop new tools, to identify Mn (co-)limitation within subpopulations of the phytoplankton community.

Conclusion

In conclusion, the signal of Mn (co-)limitation observed during these multi-seasonal experiments was masked by the strong seasonality and responses associated with Fe limitation. Our results suggest spring Fe and Mn concentrations were high enough to not limit phytoplankton growth. Conversely, phytoplankton communities were strongly Fe limited in summer. In autumn, we suggest low silicic acid levels limited diatom growth. However, the possibility that silicic acid and Fe were co-limiting diatom growth cannot be excluded. Manganese additions induced subtle community and physiological changes. In autumn, the addition of Mn alone stimulated the growth of cyanobacteria, most likely *Synechococcus* sp. These results suggest cyanobacteria may be Mn-limited in autumn when they constitute an important part of resident phytoplankton biomass and dMn concentrations are lowest following the phytoplankton growth season. In spring and summer, combined Fe and Mn additions stimulated carbon fixation in the nano- and micro- size classes, respectively. This was hypothesized to be due to the high Mn requirements of the spring community and ROS production linked to Fe limitation in summer. These results indicate that Mn may play an important role in controlling/stimulating specific phytoplankton taxa, with seasonal variability. In addition, our results show that Mn (co-)limitation signal may be hard to capture in conventional bioassays, especially when pronounced Fe responses are observed.

Acknowledgements

We would like to acknowledge the officers and crew of the RV *Investigator* (Australian Marine National Facility) for the deployment of all the instruments during the three voyages (IN2018-V04; IN2019-V02 and IN2020-V08), and the hydro-chemistry team who performed the macronutrients analyses onboard.

We thank Pamela Barrett and Robin Grun for the collection and analyses of trace metal samples performed for the first two voyages. This work was funded through the Antarctic Climate & Ecosystems Cooperative Centre (ACE CRC) and by the Australian Antarctic Program Partnership (AAPP).

References

Armstrong, F. A. 2008. "Why Did Nature Choose Manganese to Make Oxygen?" *Philosophical Transactions of the Royal Society B: Biological Sciences* 363 (1494): 1263–70. https://doi.org/10.1098/rstb.2007.2223.

Bach, L. T., Lohbeck, K. T., Reusch, T. B., and U. Riebesell. 2018. "Rapid Evolution of Highly Variable Competitive Abilities in a Key Phytoplankton Species." *Nature Ecology & Evolution* 2 (4): 611–13. https://doi.org/10.1038/s41559-018-0474-x.

Bowie, A. R., F. Griffiths, B., Dehairs, F., and T. W. Trull. 2011. "Oceanography of the Subantarctic and Polar Frontal Zones South of Australia during Summer: Setting for the SAZ-Sense Study." *Deep Sea Research Part II: Topical Studies in Oceanography* 58 (21–22): 2059–70. https://doi.org/10.1016/j.dsr2.2011.05.033.

Bowie, A. R., Lannuzel, D., Remenyi, T. A., Wagener, T., Lam, P. J., Boyd, P. W., Guieu, C., Townsend, A. T., and T. W. Trull. 2009. "Biogeochemical Iron Budgets of the Southern Ocean South of Australia: Decoupling of Iron and Nutrient Cycles in the Subantarctic Zone by the summertime supply." *Global Biogeochemical Cycles* 23 (4): n/a-n/a. https://doi.org/10.1029/2009GB003500.

Boyd, P. W., LaRoche, J., Gall, M., Frew, R., and R. M. L. McKay. 1999. "Role of Iron, Light, and Silicate in Controlling Algal Biomass in Subantarctic Waters SE of New Zealand." *Journal of Geophysical Research: Oceans* 104 (C6): 13395–408. https://doi.org/10.1029/1999JC900009.

Boyd, P. W. 2002. "Environmental factors controlling phytoplankton processes in the Southern Ocean." *Journal of Phycology* 38 (5): 844–861.

Boyd, P. W., Watson, A. J., Law, C. S., Abraham, E. R., Trull, T., Murdoch, R., Bakker, D. C. E., et al. 2000. "A Mesoscale Phytoplankton Bloom in the Polar Southern Ocean Stimulated by Iron Fertilization." *Nature* 407 (6805): 695–702. https://doi.org/10.1038/35037500.

Browning, T. J., Achterberg, E. P., Engel, A., and E. Mawji. 2021. "Manganese Co-Limitation of Phytoplankton Growth and Major Nutrient Drawdown in the Southern Ocean." *Nature Communications* 12 (1): 884. https://doi.org/10.1038/s41467-021-21122-6.

Buma, A. GJ, De Baar, H. JW, Nolting, R. F. and A. J. Van Bennekom. 1991. "Metal Enrichment Experiments in the Weddell-Scotia Seas: Effects of Iron and Manganese on Various Plankton Communities." *Limnology and Oceanography* 36 (8): 1865–1878.

Campbell, D., Hurry V., Clarke, A. K., Gustafsson, P. and G. Öquist. 1998. "Chlorophyll Fluorescence Analysis of Cyanobacterial Photosynthesis and Acclimation." *Microbiology and Molecular Biology Reviews* 62 (3): 667–83. https://doi.org/10.1128/MMBR.62.3.667-683.1998.

Cassar, N., Wright, S. W., Thomson, P. G., Trull, T. W., Westwood, K. J., de Salas, M., Davidson, A., Pearce, I., Davies, D. M. and R. J. Matear. 2015. "The Relation of Mixed-Layer Net Community Production to Phytoplankton Community Composition in the Southern Ocean." *Global Biogeochemical Cycles* 29 (4): 446–62. https://doi.org/10.1002/2014GB004936.

Deppeler, S. L. and A. T. Davidson. 2017. "Southern Ocean Phytoplankton in a Changing Climate." *Frontiers in Marine Science* 4 (February). https://doi.org/10.3389/fmars.2017.00040.

Ellwood, M. J., Strzepek, R. F., Strutton, P. G., Trull, T. W., Fourquez, M., & Boyd, P. W. (2020). Distinct iron cycling in a Southern Ocean eddy. Nature communications, 11(1), 1-8.

Eriksen, R., Trull, T. W., Davies, D., Jansen, P., Davidson, A. T., Westwood, K., and R. van den Enden. 2018. "Seasonal Succession of Phytoplankton Community Structure from Autonomous Sampling at the Australian Southern Ocean Time Series (SOTS) Observatory." *Marine Ecology Progress Series* 589 (February): 13–31. https://doi.org/10.3354/meps12420.

Ferreira, F. and N. A. Straus. 1994. "Iron Deprivation in Cyanobacteria." *Journal of Applied Phycology* 6 (2): 199–210. https://doi.org/10.1007/BF02186073.

672 Fourquez, M., Bressac, M., Deppeler, S. L., Ellwood, M., Obernosterer, I., Trull, T. W. and P. W.
673 Boyd. 2020. “Microbial Competition in the Subpolar Southern Ocean: An Fe–C Co-
674 Limitation Experiment.” *Frontiers in Marine Science* 6 (January): 776.
675 https://doi.org/10.3389/fmars.2019.00776.
676 Gao, X., Bowler, C. and E, Kazamia. 2021. “Iron Metabolism Strategies in Diatoms.” Edited by
677 Janneke Balk. *Journal of Experimental Botany* 72 (6): 2165–80.
678 https://doi.org/10.1093/jxb/eraa575.
679 Greene, R, M., Geider, R. J., Kolber, Z. and P. G. Falkowski. 1992. “Iron-Induced Changes in Light
680 Harvesting and Photochemical Energy Conversion Processes in Eukaryotic Marine Algae.”
681 *Plant Physiology* 100 (2): 565–75. https://doi.org/10.1104/pp.100.2.565.
682 Holmes, T. M., Wuttig, K., Chase, Z., Schallenberg, C., van der Merwe, P., Townsend, A. T., &
683 Bowie, A. R. (2020). Glacial and hydrothermal sources of dissolved iron (II) in Southern
684 Ocean waters surrounding Heard and McDonald Islands. Journal of Geophysical Research:
685 Oceans, 125, e2020JC016286. https://doi.org/10.1029/2020JC016286
686 Hopkinson, B. M. and K. A. Barbeau. 2008. “Interactive Influences of Iron and Light Limitation on
687 Phytoplankton at Subsurface Chlorophyll Maxima in the Eastern North Pacific.” *Limnology
688 and Oceanography* 53 (4): 1303–18. https://doi.org/10.4319/lo.2008.53.4.1303.
689 Hoppe, C.J.M., Klaas, C., Ossebaar, S., Soppa, M.A., Cheah, W., Laglera, L.M., Santos-Echeandia, J.,
690 et al. 2017. “Controls of Primary Production in Two Phytoplankton Blooms in the Antarctic
691 Circumpolar Current.” *Deep Sea Research Part II: Topical Studies in Oceanography* 138
692 (April): 63–73. https://doi.org/10.1016/j.dsr2.2015.10.005.
693 Hutchins, D. A., Sedwick, P. N., DiTullio, G. R., Boyd, P. W., Quéguiner, B., Griffiths, F. B. and C.
694 Crossley. 2001. “Control of Phytoplankton Growth by Iron and Silicic Acid Availability in
695 the Subantarctic Southern Ocean: Experimental Results from the SAZ Project.” *Journal of
696 Geophysical Research: Oceans* 106 (C12): 31559–72. https://doi.org/10.1029/2000JC000333.
697 Jackson, G. A. 2005. “Role of Algal Aggregation in Vertical Carbon Export during SOIREE and in
698 Other Low Biomass Environments.” *Geophysical Research Letters* 32 (13): L13607.
699 https://doi.org/10.1029/2005GL023180.
700 Koblıžek, M., Kaftan, D. and L. Nedbal. 2001. “On the Relationship between the Non-Photochemical
701 Quenching of the Chlorophyll Fluorescence and the Photosystem II Light Harvesting
702 Efficiency. A Repetitive Flash Fluorescence Induction Study,” 12.
703 Marie, D., Partensky, F., Vaulot, D. and C. Brussaard. 1999. “Enumeration of Phytoplankton,
704 Bacteria, and Viruses in Marine Samples.” *Current Protocols in Cytometry* 10 (1).
705 https://doi.org/10.1002/0471142956.cy1111s10.
706 Moore, C. M. 2013. “Processes and Patterns of Oceanic Nutrient Limitation.” *Nature Geosciences.* 6:
707 10.
708 Ohnemus, D. C., Krause, J. W., Brzezinski, M. A., Collier, J. L., Baines, S. B. and B. S. Twining.
709 2018. “The Chemical Form of Silicon in Marine Synechococcus.” *Marine Chemistry* 206
710 (October): 44–51. https://doi.org/10.1016/j.marchem.2018.08.004.
711 Paasche, E. 1973. “Silicon and the Ecology of Marine Plankton Diatoms. I. Thalassiosira Pseudonana
712 (Cyclotella Nana) Grown in a Chemostat with Silicate as Limiting Nutrient.” *Marine Biology*
713 19 (2): 117–26. https://doi.org/10.1007/BF00353582.
714 Peers, G. and N. M. Price. 2004. “A Role for Manganese in Superoxide Dismutases and Growth of
715 Iron-Deficient Diatoms.” *Limnology and Oceanography* 49 (5): 1774–83.
716 https://doi.org/10.4319/lo.2004.49.5.1774.
717 Perron, M.G., Proemse, B. C., Strzelec, M., Gault-Ringold, M., Boyd, P. W., Sanz Rodriguez, E.,
718 Paull, B. and A. R. Bowie. 2020. “Origin, Transport and Deposition of Aerosol Iron to
719 Australian Coastal Waters.” *Atmospheric Environment* 228 (May): 117432.
720 https://doi.org/10.1016/j.atmosenv.2020.117432.
721 Petrou, K., Hassler, C. S., Doblin, M. A., Shelly, K., Schoemann, V., van den Enden, R., Wright, S.
722 and P. J. Ralph. 2011. “Iron-Limitation and High Light Stress on Phytoplankton Populations
723 from the Australian Sub-Antarctic Zone (SAZ).” *Deep Sea Research Part II: Topical Studies
724 in Oceanography* 58 (21–22): 2200–2211. https://doi.org/10.1016/j.dsr2.2011.05.020.
725 R Core Team (2020). R: A language and environment for statistical computing. R Foundation for
726 Statistical Computing, Vienna, Austria. URL https://www.R-project.org/

Rees, C., Pender, L., Sherrin, K., Schwanger, C., Hughes, P., Tibben, S., Marouchos, A. and Mark Rayner. 2018. “Methods for Reproducible Shipboard SFA Nutrient Measurement Using RMNS and Automated Data Processing.” *Limnology and Oceanography: Methods*, December. https://doi.org/10.1002/lom3.10294.

Rintoul, S. R. and T. W. Trull. 2001a. “Seasonal Evolution of the Mixed Layer in the Subantarctic Zone South of Australia.” *Journal of Geophysical Research: Oceans* 106 (C12): 31447–62. https://doi.org/10.1029/2000JC000329.

Salomon, E. and N. Keren. 2011. “Manganese Limitation Induces Changes in the Activity and in the Organization of Photosynthetic Complexes in the Cyanobacterium *Synechocystis* Sp. Strain PCC 6803.” *Plant Physiology* 155 (1): 571–79. https://doi.org/10.1104/pp.110.164269.

Scharek, R., Van Leeuwe, M. A., and H. JW De Baar. 1997. “Responses of Southern Ocean Phytoplankton to the Addition of Trace Metals.” *Deep Sea Research Part II: Topical Studies in Oceanography* 44 (1–2): 209–227.

Sedwick, P. N., DiTullio, G. R., Hutchins, D. A., Boyd, P. W., Griffiths, F. B., Crossley, A. C., Trull, T. W. and B. Quéguiner. 1999. “Limitation of Algal Growth by Iron Deficiency in the Australian Subantarctic Region.” *Geophysical Research Letters* 26 (18): 2865–68. https://doi.org/10.1029/1998GL002284.

Sedwick, P. N., DiTullio, G. R. and D. J. Mackey. 2000. “Iron and Manganese in the Ross Sea, Antarctica: Seasonal Iron Limitation in Antarctic Shelf Waters.” *Journal of Geophysical Research: Oceans* 105 (C5): 11321–36. https://doi.org/10.1029/2000JC000256.

Sedwick, P.N., Bowie, A.R. and T.W. Trull. 2008. “Dissolved Iron in the Australian Sector of the Southern Ocean (CLIVAR SR3 Section): Meridional and Seasonal Trends.” *Deep Sea Research Part I: Oceanographic Research Papers* 55 (8): 911–25. https://doi.org/10.1016/j.dsr.2008.03.011.

Strzepek, R. F., Maldonado, M. T., Hunter, K. A., Frew, R. D. and P. W. Boyd. 2011. “Adaptive Strategies by Southern Ocean Phytoplankton to Lessen Iron Limitation: Uptake of Organically Complexed Iron and Reduced Cellular Iron Requirements.” *Limnology and Oceanography* 56 (6): 1983–2002. https://doi.org/10.4319/lo.2011.56.6.1983.

Suggett, D. J., MacIntyre, H. L. and R. J. Geider. 2004. “Evaluation of Biophysical and Optical Determinations of Light Absorption by Photosystem II in Phytoplankton: Evaluation of Light Absorption by PSII.” *Limnology and Oceanography: Methods* 2 (10): 316–32. https://doi.org/10.4319/lom.2004.2.316.

Suggett, D. J., Moore, C. M., Hickman, A. E., and R. J. Geider. 2009. “Interpretation of Fast Repetition Rate (FRR) Fluorescence: Signatures of Phytoplankton Community Structure versus Physiological State.” *Marine Ecology Progress Series* 376 (February): 1–19. https://doi.org/10.3354/meps07830.

Sunda, W. G. and S. A. Huntsman. 1995. “Iron Uptake and Growth Limitation in Oceanic and Coastal Phytoplankton.” *Marine Chemistry* 50 (1–4): 189–206. https://doi.org/10.1016/0304-4203(95)00035-P.

Twining, B. S., Baines, S. B. and N. S. Fisher. 2004. “Element Stoichiometries of Individual Plankton Cells Collected during the Southern Ocean Iron Experiment (SOFeX).” *Limnology and Oceanography* 49 (6): 2115–28. https://doi.org/10.4319/lo.2004.49.6.2115.

Twining, B. S., Nuñez-Milland, D., Vogt, S., Johnson, R. S. and P. N. Sedwick. 2010. “Variations in *Synechococcus* Cell Quotas of Phosphorus, Sulfur, Manganese, Iron, Nickel, and Zinc within Mesoscale Eddies in the Sargasso Sea.” *Limnology and Oceanography* 55 (2): 492–506. https://doi.org/10.4319/lo.2010.55.2.0492.

Waite, A. M., Safi, K. A., Hall, J. A. and S. D. Nodder. 2000. “Mass Sedimentation of Picoplankton Embedded in Organic Aggregates.” *Limnology and Oceanography* 45 (1): 87–97. https://doi.org/10.4319/lo.2000.45.1.0087.

Westwood, K. J., F. Griffiths, B., Webb, J. P. and S. W. Wright. 2011. “Primary Production in the Sub-Antarctic and Polar Frontal Zones South of Tasmania, Australia; SAZ-Sense Survey, 2007.” *Deep Sea Research Part II: Topical Studies in Oceanography* 58 (21–22): 2162–78. https://doi.org/10.1016/j.dsr2.2011.05.017.

780 Wolfe-Simon, F., Starovoytov, V., Reinfelder, J. R., Schofield, O. and P. G. Falkowski. 2006.
781 "Localization and Role of Manganese Superoxide Dismutase in a Marine Diatom." *Plant*
782 *Physiology* 142 (4): 1701–9. https://doi.org/10.1104/pp.106.088963.
783 Wu, M., McCain, J. S. P., Rowland, E., Middag, R., Sandgren, M., Allen, A. E. and E. M. Bertrand.
784 2019. "Manganese and Iron Deficiency in Southern Ocean Phaeocystis Antarctica
785 Populations Revealed through Taxon-Specific Protein Indicators." *Nature Communications*
786 10 (1): 3582. https://doi.org/10.1038/s41467-019-11426-z.
787